J|A|C|S COMMUNICATIONS

Published on Web 10/13/2010

Single-Crystal Colloidal Nanosheets of GeS and GeSe

Dimitri D. Vaughn II,[†] Romesh J. Patel,[‡] Michael A. Hickner,[‡] and Raymond E. Schaak*[,†,§]

Department of Chemistry, Department of Materials Science and Engineering, and Materials Research Institute, The Pennsylvania State University, University Park, Pennsylvania 16802, United States

Received August 19, 2010; E-mail: schaak@chem.psu.edu

Abstract: Narrow-band-gap IV−VI semiconductors offer promising optoelectronic properties for integration as light-absorbing components in field-effect transistors, photodetectors, and photovoltaic devices. Importantly, colloidal nanostructures of these materials have the potential to substantially decrease the fabrication cost of solar cells because of their ability to be solution-processed. While colloidal nanomaterials formed from IV−VI lead chalcogenides such as PbS and PbSe have been extensively investigated, those of the layered semiconductors SnS, SnSe, GeS, and GeSe have only recently been considered. In particular, there have been very few studies of the germanium chalcogenides, which have band-gap energies that overlap well with the solar spectrum. Here we report the first synthesis of colloidal GeS and GeSe nanostructures obtained by heating GeI_4, hexamethyldisilazane, oleylamine, oleic acid, and dodecanethiol or trioctylphosphine selenide to 320 °C for 24 h. These materials, which were characterized by TEM, SAED, SEM, AFM, XRD, diffuse reflectance spectroscopy, and *I*−*V* conductivity measurements, preferentially adopt a two-dimensional single-crystal nanosheet morphology that produces fully [100]-oriented films upon drop-casting. Optical measurements indicated indirect band gaps of 1.58 and 1.14 eV for GeS and GeSe, respectively, and electrical measurements showed that drop-cast films of GeSe exhibit p-type conductivity.

Narrow-band-gap IV−VI semiconductors constitute an important class of materials for photovoltaic applications.[1−3] These materials typically have band gaps in the range 0.5−1.5 eV, making them efficient absorbers of incident solar radiation. In addition, IV−VI semiconductors have been shown to exhibit multiple exciton generation, which can lead to improved solar cell efficiencies.[4−6] Among these compounds, there is growing interest in the layered semiconductors SnS, SnSe, GeS, and GeSe,[7−13] which are predicted to have high chemical and environmental stability and show promise as low-cost components of photovoltaic cells. Furthermore, they consist of more environmentally friendly elements than alternative narrow-band-gap systems containing Pb, Cd, and Hg. GeS and GeSe, which are orthorhombic with a distorted rock-salt structure, have both indirect and direct band gaps that are closely spaced in energy. For GeS, the direct and indirect band gaps have been reported to be in the range 1.55−1.65 eV,[13] and for GeSe, they are in the range 1.1−1.2 eV.[12] There have been several reports of colloidal routes to SnS and SnSe nanoparticles.[7−10] However, despite the fact that their band-gap energies overlap fairly well with the solar spectrum, the Ge analogues have not previously been reported as colloidal nanostructures.

Here we report a simple one-pot solution-chemistry route to colloidal nanostructures of GeS and GeSe. Importantly, we have found that the GeS and GeSe systems form single-crystal nanosheets similar to those of graphene and other layered materials, including metal oxides and chalcogenides.[14−17] Such colloidal nanostructures are optimal for solution-based processing techniques such as spin-coating, dip-coating, and inkjet printing, which permit cheaper fabrication of photovoltaic devices.[1,3,4] Colloidal nanosheets in particular can serve as building blocks for the design of novel nanocomposites and sophisticated lamellar nanostructures with enhanced photovoltaic efficiencies.[18−20]

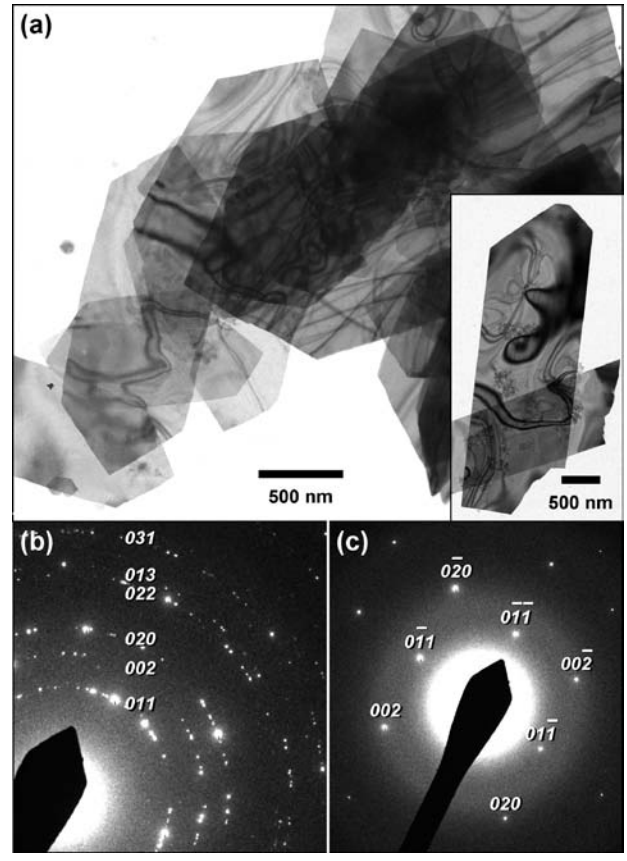

Figure 1. (a) TEM images of GeS and (inset) GeSe nanosheets. (b) SAED pattern for a polycrystalline sample of GeS nanosheets. (c) SAED pattern corresponding to a single [100]-oriented GeS nanosheet.

Colloidal nanosheets of GeS were synthesized by mixing GeI_4 (60 mg), hexamethyldisilazane (HMDS, 1 mL), oleylamine (10 mL), oleic acid (0.75 mL), and dodecanethiol (0.5 mL) at room temperature followed by heating to 320 °C for ∼24 h. The use of dodecanethiol as a suitable sulfur source has been reported previously in the synthesis of the sulfides of other metals, including

[†] Department of Chemistry.
[‡] Department of Materials Science and Engineering.
[§] Materials Research Institute.

10.1021/ja107520b

Cu, Pb, and Zn,[21] and avoids the use of toxic, pyrophoric, and expensive alkylphosphines. GeSe nanosheets were synthesized using an identical procedure except that trioctylphosphine selenide (TOPSe) was used as the selenium source.

Figure 1a and Figure S1 in the Supporting Information show representative transmission electron microscopy (TEM) images of the GeS and GeSe nanosheets. The nanosheets appear mostly as elongated hexagons with average lateral dimensions of 2−4 μm × 0.5−1 μm. Scanning electron microscopy (SEM) and atomic force microscopy (AFM) images were used to confirm the nanosheet morphology (Figures S2−S4). For GeS, AFM images indicated an average nanosheet thickness of 5 nm with a range that spanned 3−20 nm (Figure S3), and the sheet morphology was confirmed by powder X-ray diffraction (XRD) data showing *h*00 peaks that were broader than the other *hk*0, *h*0*l*, 0*kl*, and *hkl* reflections (Figure S4). For GeSe, a larger range of thicknesses was observed using SEM (5−100 nm), with most larger than 20 nm (Figure S2). For both GeS and GeSe, selected-area electron diffraction (SAED) experiments produced polycrystalline ring patterns consistent with nanosheets having the orthorhombic GeS-type structure (Figure 1b). The observed rings correspond to the 0*kl* set of reflections, indicating that the sheets are oriented along [100]. When the electron beam was focused on individual nanosheets, a spot pattern was observed (Figure 1c and Figure S1), and this is also consistent with [100]-oriented GeS and GeSe nanosheets.

Figure 2 shows powder XRD patterns for the GeS and GeSe products. Both powders appeared to be phase-pure as determined by XRD, and their XRD patterns matched well with simulated patterns based on their known orthorhombic GeS-type structure. The lattice constants also agreed well with literature values:[22,23] for GeS, a = 10.52 Å, b = 3.65 Å, and c = 4.30 Å ($a_{\mathrm{lit,GeS}}$ = 10.47 Å, $b_{\mathrm{lit,GeS}}$ = 3.64 Å, and $c_{\mathrm{lit,GeS}}$ = 4.30 Å), and for GeSe, a = 10.78 Å, b = 3.81 Å, and c = 4.37 Å ($a_{\mathrm{lit,GeSe}}$ = 10.83 Å, $b_{\mathrm{lit,GeSe}}$ = 3.83 Å, and $c_{\mathrm{lit,GeSe}}$ = 4.39 Å). When the colloidal suspensions of nanosheets were drop-cast onto planar substrates rather than being collected as largely isotropic aggregated powders, the resulting XRD patterns showed perfect preferred orientation, with only the *h*00 reflections evident. This indicates that the bulk samples consist almost entirely of [100]-oriented nanosheets.

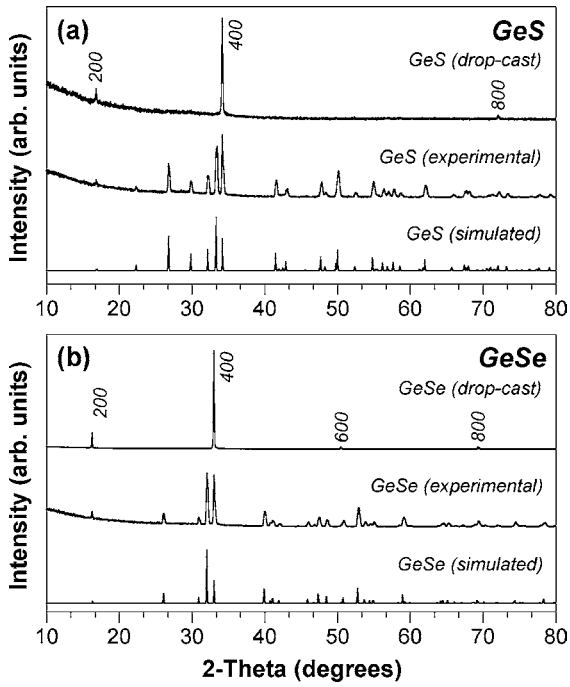

Figure 2. Powder XRD patterns for (a) GeS and (b) GeSe nanosheets. In both (a) and (b), patterns for simulated and experimental polycrystalline samples as well as [100]-oriented samples prepared by drop casting are shown.

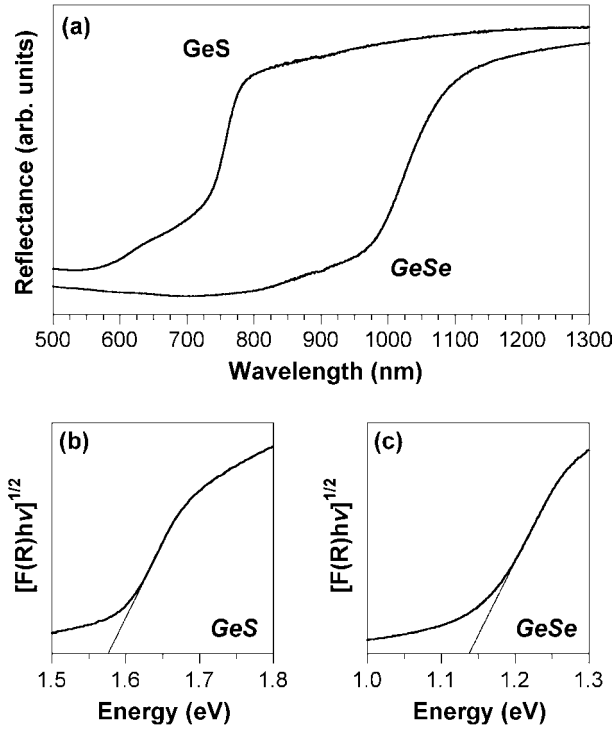

Figure 3. (a) Diffuse reflectance spectra for GeS and GeSe nanosheets. (b, c) Plots of $[F(R)h\nu]^{1/2}$ vs energy for the (b) GeS and (c) GeSe nanosheets, from which indirect band-gap energies were obtained.

Diffuse reflectance spectroscopy was used to investigate the optical properties of the GeS and GeSe nanosheets. As shown in Figure 3a, the onset of absorption for the GeS sheets began near 800 nm, while for GeSe, the absorption onset began near 1150 nm. These transitions were used to estimate both the indirect and direct band gaps by performing Kubelka−Munk transformations.[24] For GeS, a plot of $[F(R)h\nu]^{1/2}$ versus energy (Figure 3b) yielded an indirect band gap of 1.58 eV, and a plot of $[F(R)h\nu]^2$ versus energy (Figure S5a) yielded a direct band gap of 1.61 eV. The band structure of GeS is complex, with multiple competing band gaps of similar energy.[13] Previous reports have indicated band gaps in the range 1.55−1.65 eV,[25,26] which are consistent with what we observed. For the GeSe nanosheets, Kubelka−Munk plots (Figure 3c and Figure S5b) indicated indirect and direct band gaps of 1.14 and 1.21 eV, respectively. These values match well with previously reported results for GeSe.[27,28]

The electrical transport properties of the GeSe nanosheets as a representative system were studied. The GeSe nanosheets were drop-cast onto a four-point gold electrode pad (Figure S7) from a methanol slurry to form a 74 μm thick film. The film was dried under ambient conditions for 6 h, and four-point $I-V$ measurements (Figure 4a) were performed. The conductivity of the film (normalized for geometry) was calculated to be 4.7×10^{-6} S cm^{-1}, which is in reasonable agreement with values for films made using other colloidal narrow-band-gap semiconductors.[1,10] Furthermore, the two-point $I-V$ plot (Figure 4b) showed turn-on potentials of −6.5 and +10 V in the negative and positive quadrants, respectively, suggesting a p-type character. The $I-V$ data confirmed that

conductive solid-state films of [100]-oriented GeSe can be produced by simple drop-casting of as-synthesized colloidal GeSe nanosheet suspensions.

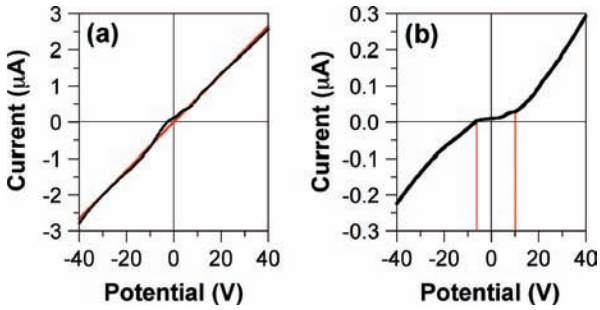

Figure 4. *I*−*V* plots for GeSe nanosheet films: (a) four-point *I*−*V* curve (black) and the linear fit used for the conductivity calculation (red); (b) two-point *I*−*V* curve with turn-on potentials denoted (red lines).

In conclusion, single-crystal colloidal nanosheets of the narrow-band-gap semiconductors GeS and GeSe have been synthesized using a simple one-pot strategy. The nanosheets can be solution-processed into [100]-oriented films, and their band gaps provide good overlap with the solar spectrum. Coupled with previously reported electrical measurements of single GeSe sheets made using a vapor−condensation−recrystallization process,[11] the nanosheet morphologies, band-gap energies, and conductivities make the GeS and GeSe nanostructures promising for use as light-absorption layers in Shockley−Queisser-limited solar cells[4] as well as other nanoelectronic devices, including photoconducting cells, p−n junctions, and field-effect transistors.[15]

Acknowledgment. This work was supported primarily by the U.S. Department of Energy, Office of Basic Energy Sciences, Division of Materials Sciences and Engineering, under Award #DE-FG02-08ER46483 (R.E.S., materials synthesis and characterization. D.D.V. acknowledges partial support from the Bunton-Waller Fellows Program, an NSF Graduate Research Fellowship, and the Research Corporation Scialog Program. TEM and SEM were performed in the Electron Microscopy Facility of the Huck Institutes of the Life Sciences. The authors thank Josh Stapleton and Tad Daniels at the Penn State Materials Characterization Laboratory for help with the diffuse reflectance and AFM measurements, respectively.

Supporting Information Available: Complete experimental details and additional TEM, SEM, AFM, XRD, SAED, and diffuse-reflectance data. This material is available free of charge via the Internet at http://pubs.acs.org.

References

(1) Talapin, D. V.; Lee, J. S.; Kovalenko, M. V.; Shevchenko, E. V. *Chem. Rev.* **2010**, *110*, 389.
(2) Sargent, E. H. *Adv. Mater.* **2005**, *17*, 515.
(3) Sargent, E. H. *Nat. Photonics* **2009**, *3*, 332.
(4) Hillhouse, H. W.; Beard, M. C. *Curr. Opin. Colloid Interface Sci.* **2009**, *14*, 245.
(5) Rogach, A. L.; Eychmuller, A.; Hickey, S. G.; Kershaw, S. V. *Small* **2007**, *3*, 536.
(6) Ellingson, R. J.; Beard, M. C.; Johnson, J. C.; Yu, P. R.; Micic, O. I.; Nozik, A. J.; Shabaev, A.; Efros, A. L. *Nano Lett.* **2005**, *5*, 865.
(7) Xu, Y.; Al-Salim, N.; Bumby, C. W.; Tilley, R. D. *J. Am. Chem. Soc.* **2009**, *131*, 15990.
(8) Hickey, S. G.; Waurisch, C.; Rellinghaus, B.; Eychmuller, A. *J. Am. Chem. Soc.* **2008**, *130*, 14978.
(9) Franzman, M. A.; Schlenker, C. W.; Thompson, M. E.; Brutchey, R. L. *J. Am. Chem. Soc.* **2010**, *132*, 4060.
(10) Baumgardner, W. J.; Choi, J. J.; Lim, Y. F.; Hanrath, T. *J. Am. Chem. Soc.* **2010**, *132*, 9519.
(11) Yoon, S. M.; Song, H. J.; Choi, H. C. *Adv. Mater.* **2010**, *22*, 2164.
(12) Makinistian, L.; Albanesi, E. A. *J. Phys.: Condens. Matter* **2007**, *19*, 186211.
(13) Makinistian, L.; Albanesi, E. A. *Phys. Rev. B* **2006**, *74*, 045206.
(14) Rao, C. N. R.; Sood, A. K.; Subrahmanyam, K. S.; Govindaraj, A. *Angew. Chem., Int. Ed.* **2009**, *48*, 7752.
(15) Osada, M.; Sasaki, T. *J. Mater. Chem.* **2009**, *19*, 2503.
(16) Seo, J. W.; Jun, Y. W.; Park, S. W.; Nah, H.; Moon, T.; Park, B.; Kim, J. G.; Kim, Y. J.; Cheon, J. *Angew. Chem., Int. Ed.* **2007**, *46*, 8828.
(17) Oyler, K.; Ke, X.; Sines, I. T.; Schiffer, P.; Schaak, R. E. *Chem. Mater.* **2009**, *21*, 3655.
(18) Kaschak, D. M.; Lean, J. T.; Waraska, C. C.; Saupe, G. B.; Usami, H.; Mallouk, T. E. *J. Am. Chem. Soc.* **1999**, *121*, 3435.
(19) Li, L.; Ma, R.; Ebina, Y.; Fukuda, K.; Takada, K.; Sasaki, T. *J. Am. Chem. Soc.* **2007**, *129*, 8000.
(20) Compton, O. C.; Mullet, C. H.; Chiang, S.; Osterloh, F. E. *J. Phys. Chem. C* **2008**, *112*, 6202.
(21) Choi, S. H.; An, K.; Kim, E. G.; Yu, J. H.; Kim, J. H.; Hyeon, T. *Adv. Funct. Mater.* **2009**, *19*, 1645.
(22) Bissert, V. G.; Hesse, K. F. *Acta Crystallogr.* **1978**, *34*, 1322.
(23) Wiedemeier, H.; Schnering, H. G. V. *Z. Kristallogr.* **1978**, *148*, 295.
(24) Hagfeldt, A.; Grätzel, M. *Chem. Rev.* **1995**, *95*, 49.
(25) Elkorashy, A. M. *J. Phys.: Condens. Matter* **1990**, *2*, 6195.
(26) Elkorashy, A. M. *J. Phys. C: Solid State Phys.* **1988**, *21*, 2595.
(27) Elkorashy, A. M. *Phys. Status Solidi B* **1989**, *152*, 249.
(28) Elkorashy, A. M. *Phys. Status Solidi B* **1986**, *135*, 707.

JA107520B